Journal of Computational Science 5 (2014) 841–846

Contents lists available at ScienceDirect

Journal of Computational Science

journal homepage: www.elsevier.com/locate/jocs

Bridging the gap: From cellular automata to differential equation models for pedestrian dynamics

Felix Dietrich[a,b,*], Gerta Köster[a], Michael Seitz[a,b], Isabella von Sivers[a,b]

[a] Munich University of Applied Sciences, Lothstr. 64, 80335 München, Germany
[b] Technische Universität München, Boltzmannstr. 3, 85747 Garching, Germany

ARTICLE INFO

Article history:
Received 30 November 2013
Received in revised form 18 May 2014
Accepted 1 June 2014
Available online 9 June 2014

Keywords:
Cellular automata
Ordinary differential equation
Pedestrian dynamics
Optimal Steps Model
Gradient Navigation Model

ABSTRACT

Cellular automata (CA) and ordinary differential equation (ODE) models compete for dominance in microscopic pedestrian dynamics. There are two major differences: movement in a CA is restricted to a grid and navigation is achieved by moving directly in the desired direction. Force based ODE models operate in continuous space and navigation is computed indirectly through the acceleration vector. We present the Optimal Steps Model and the Gradient Navigation Model, which produce trajectories similar to each other. Both are grid-free and free of oscillations, leading to the conclusion that the two major differences are also the two major weaknesses of the older models.

1. Introduction

Several approaches for modeling microscopic pedestrian dynamics have been developed in the last decades [37,5]. Among these, two compete for supremacy: cellular automata (CA) and models based on ordinary differential equations (ODE). In typical formulations, both model types use the idea that pedestrians are driven by repulsive and attractive forces. Other pedestrians and obstacles repel, targets attract. However, the mathematical formulations differ fundamentally, especially as far as treatment of space and navigation is concerned.

In CA [3,16,14,9,36], the given area is divided into cells of equal shape and area that are either empty or occupied by a pedestrian, a target or an obstacle. This status is updated at each time step, that is, virtual pedestrians move from cell to cell according to certain rules. Typically, the pedestrians navigate along a floor field that expresses attraction and repulsion acting on the pedestrians [11,17]. In most CA-models, acceleration to each pedestrian's free-flow velocity is achieved instantaneously if there is space to move. The coarse discretization of space limits the choice of direction and influences space requirements and the handling of speed [17]. Advantages are high computational speed, simplicity, as well as easy and intuitive integration of rules governing pedestrian behavior.

ODE-models for pedestrian motion are usually inspired by Newtonian mechanics. They also consider attractive and repulsive forces but operate in continuous space and time. Navigation is realized indirectly by computing an acceleration vector from a superposition of forces. Acceleration is delayed by a friction term. The best known ODE-model is the Social Force Model (SFM) introduced by Dirk Helbing and Péter Molnár in 1995 [13]. Problems of this ansatz include a treatment of inertia that is often inappropriate for pedestrian dynamics [4] as well as numerical pitfalls [19]. Furthermore, typical or specific behavior of pedestrians, even prevention of overlapping, can only be achieved by introducing extra complexity [6,5].

In this paper, we present and compare two new models that remove the major differences between the CA and ODE models: First, the Optimal Steps Model [27,32], which remains rule based as a CA but allows movement in continuous space. Second, the Gradient Navigation Model [8], which uses ordinary differential equations like the SFM but computes velocity, and hence direction of movement, directly from the forces. See Fig. 1 for a schematic representation of how to bridge the gap between CA and ODE models. Both approaches maintain the advantages of the models they were inspired by, but do not suffer from the main disadvantages. They are robust and successfully validated according to the guidelines given in [25]. Both can be calibrated to a given fundamental diagram [8,32]. Numerical experiments yield very similar trajectories showing that they are indeed more alike than the original CA and ODE models. See Section 4.

* Corresponding author. Tel.: +49 8912653762.
E-mail address: felix.dietrich@tum.de (F. Dietrich).

http://dx.doi.org/10.1016/j.jocs.2014.06.005
1877-7503/

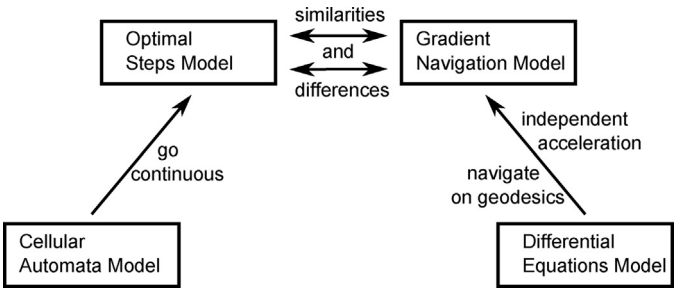

Fig. 1. Bridging the gap between CA- and DE-models.

The paper is structured as follows: in Sections 2 and 3 we briefly introduce the two new models stating their main ideas and underline where they deviate from the CA and social force approaches. For detailed descriptions we refer to the original publications [27,32,8]. Then we show the results of numerical experiments for all four model types to support our hypothesis that the two new models do not only perform better but produce similar results (Section 4). In Section 5 we discuss which differences remain. In the conclusion section (Section 6) we propose desirable next steps.

2. Optimal Steps Model

In this section we give an outline of the Optimal Steps Model (OSM) as it is described in [27] and enhanced in [32]. The model is inspired by the idea that pedestrians try to optimize their position in space according to a balance of goals: reaching the target and avoiding obstacles and other pedestrians. This approach is also used for cellular automata models of pedestrian movement [18] and the discrete choice framework described in [1]. Virtual pedestrians move by locally minimizing a scalar field $P : \mathbb{R}^2 \to \mathbb{R}$ that maps each position to a value that is computed as a superposition of potentials: attraction by targets and repulsion by other pedestrians and obstacles. The aggregated potential for each pedestrian serves as an objective function to find the optimal position on a disc around the current position of the pedestrian (see Fig. 2). The radius of the disc is the stride length that corresponds to each pedestrian's individual free-flow velocity. Thus, stepping forward has become a non-linear optimization problem in continuous space. As a result, pedestrians can make adjusting steps that are shorter than the free-flow stride length, thus naturally slowing down in dense situations when navigation becomes difficult (see Fig. 3). Calibration to a given density–velocity profile is achieved by adjusting the repulsive potentials of pedestrians and obstacles [32]. Single steps can still be distinguished in the trajectories (see Fig. 3). That is why we call

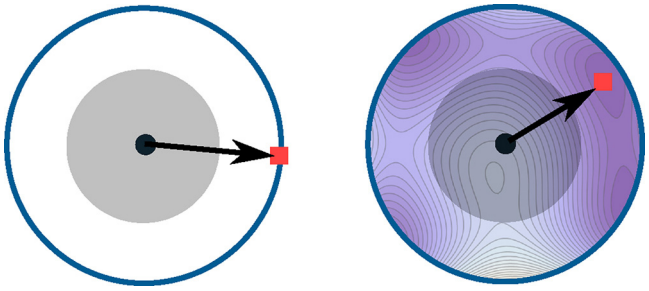

Fig. 2. The two step types in the OSM: The gray region shows a pedestrian torso with its center. The individual stride length is given by the solid (blue) circular line. The square displays the minimum of the aggregated potential for the pedestrian and hence the next position. On the left, it is on the circular line, that is, the pedestrian strides freely. On the right, the next position is within the circle. (For interpretation of the references to color in this figure legend, the reader is referred to the web version of this article.)

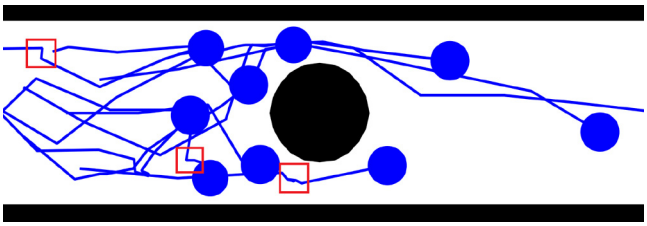

Fig. 3. Pedestrians simulated by the OSM move simultaneously from left to right along a corridor with a column placed in the middle. They make small, sometimes evasive, steps as highlighted by the (red) rectangles. Once the obstacle has been passed, the stride length increases and the pedestrians resume their free-flow velocity. (For interpretation of the references to color in this figure legend, the reader is referred to the web version of this article.)

the model quasi-continuous. In contrast to a CA, the pedestrians are not fixed to cells, but can reach every location in the observed area. Discretization has become a dynamic process governed by natural stepping behavior, which represents a natural discretization of pedestrian movement.

If we restrict the optimization to positions on the circle, instead of on the whole disc, and allow only six equidistant positions on the circle, a hexagonal CA grid is reproduced. With four positions on one circle or two circles with four positions on each, we get rectangular CA grids with von-Neumann or Moore neighborhoods [27].

2.1. Potential

A very successful way to compute a target potential is to compute the arrival time of a wave front propagating from the target and thereby skirting obstacles. As a result, pedestrians navigate along geodesics [33,11] and around obstacles. Navigation around obstacles with a floor field has also been used in earlier models based on a Manhattan metric [3,24]. Let $\Omega \subset \mathbb{R}^2$ be the area of the scenario and $\Gamma \subset \partial\Omega$ the boundary of the target region. Then the Eikonal equation defines the arrival time $\sigma : \Omega \to \mathbb{R}$ of a wave front propagating with speed $F(x)$:

$$\begin{aligned} F(x)\|\nabla\sigma(x)\| &= 1 \qquad \text{for } x \in \Omega \\ \sigma(x) &= 0 \qquad \text{for } x \in \Gamma. \end{aligned} \tag{1}$$

We compute its numerical solution σ_N by Sethian's Fast Marching algorithm on a two-dimensional grid [28,29]. Between the distinct values of the grid, σ_N is interpolated bilinearly [11,27] to $\tilde{\sigma_N}$ in the OSM. Thus the target potential $P_t(x) = \tilde{\sigma_N}(x)$ is given for each point $x \in \Omega$. In addition to the target potential, the aggregated potential $P_i(x)$ at a given point $x \in \Omega$ is composed of pedestrian potentials and obstacle potentials [27]. The pedestrian potential $P_p^j(x)$ is generated by pedestrian j. It only depends on the Euclidean distance between the center of pedestrian j and the considered position x in the scenario. The obstacle potential is very similar to the pedestrian potential. Here, the obstacle potential $P_o^k(x)$ for obstacle k depends on the Euclidean distance between the considered position x and the nearest point of the obstacle to x.

For each pedestrian i in a scenario with n pedestrians and m obstacles

$$P_i(x) = P_t(x) + \sum_{j=1, j\neq i}^{n} P_p^j(x) + \sum_{k=1}^{m} P_o^k(x), \tag{2}$$

assigns the aggregated potential $P_i(x)$ to an arbitrary point $x \in \Omega$ [27].

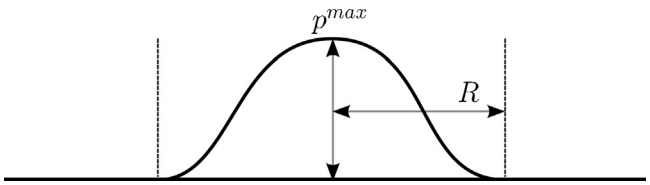

Fig. 4. The norm of ∇P_p^j, which is determined by its maximum p^{max}/e and support $2R$ (see [8]).

3. Gradient Navigation Model

The Gradient Navigation Model (GNM) is composed of a set of ordinary differential equations to determine the position of each pedestrian x_i in two dimensional space as well as the scalar speed and navigational direction [8]. The idea is to compute the velocity vector as the gradient of several distance dependent, scalar functions similar to P_i in the OSM (see Eq. (2)). This constitutes a strong deviation from Newtonian dynamics and hence from the Social Force Model [13], where the acceleration vector is computed from the forces. Models using velocity obstacles also compute the velocity vector directly but focus more on a collision-free trajectory for robots [10,31,2,7].

The change in position of pedestrians is not instantaneous. We follow [22] and assume a certain time delay. We model the resulting relaxed speed adaptation by a multiplicative, time dependent, scalar variable w, which we call relaxed speed. Its derivative with respect to time, $\dot{w}$, is similar to acceleration and depends on the relaxation constant τ.

In the Gradient Navigation Model, the equations of motion for a pedestrian i are given by

$$\begin{aligned} \dot{\vec{x}}_i(t) &= w_i(t)\vec{N}(\vec{x}_i, t) \\ \dot{w}_i(t) &= \frac{1}{\tau}\left(v_i(\rho(\vec{x}_i))\|\vec{N}(\vec{x}_i, t)\| - w_i(t)\right) \end{aligned} \tag{3}$$

with navigation function $\vec{N}$

$$\vec{N}(\vec{x}_i, t) = -g\left(g(\nabla\sigma(\vec{x}_i)) + g(\nabla\delta(\vec{x}_i, t))\right) \tag{4}$$

and initial conditions $\vec{x}_{i0} = \vec{x}_i(0)$ and $w_{i0} = w_i(0)$. The gradients of the functions σ and δ are used to steer pedestrians to the target and away from other pedestrians. Together with $v(\rho)$, they are defined below. The function $g : \mathbb{R}^2 \to \mathbb{R}^2$ scales the length of a given vector to lie in the interval $[0, 1]$. For the exact formula see [8]. The position $\vec{x} : \mathbb{R} \to \mathbb{R}^2$ and the one-dimensional relaxed speed $w : \mathbb{R} \to \mathbb{R}$ are functions of time t.

The individuals' desired speed is represented by $v_i(\rho(\vec{x}_i))$, which can be chosen to enforce additional deceleration in a dense crowd as observed by [15]. Note that this does not lead to an exact match of the simulated speed-density relation with the fundamental diagram. Even with $v_i(\rho(\vec{x}_i)) = v_i$ constant as chosen in this paper, pedestrians in the GNM slow down when they approach others. When getting too close to one another, the gradients of the pedestrians in front cancel out the target gradient and movement stops.

Both σ and δ are closely related to the potential functions of the OSM described in Eq. (2). The first arrival time to the closest target region around static obstacles is again given by $\sigma : \Omega \to \mathbb{R}$ from Eq. (1) and again solved with the Fast Marching algorithm to yield σ_N. To get a smooth gradient $\nabla\sigma$, we employ mollification theory [8] rather than bilinear smoothing as in the OSM.

The gradients of all distance functions of all other pedestrians and walls are combined and form $\nabla\delta$:

$$\nabla\delta_i(x) = \sum_{j=1, j\neq i}^{n} \nabla P_p^j(x) + \sum_{k=1}^{m} \nabla P_o^k(x) \tag{5}$$

With these equations, the direction of pedestrian i changes independently of physical constraints, similar to the idea of a heuristic by [23] and the Optimal Steps Model [27,32]. The norm of the navigation function N and the relaxed speed w determines the speed $\dot{x}$ in the desired direction.

The norm of the gradients ∇P_p^j and ∇P_o^k resemble the monotonically decreasing function used for the potential values in the OSM. To ensure smoothness of the derivatives, we choose a smooth exponential function with compact support:

$$\|\nabla P_p^j\| = \begin{cases} p^{\max}\exp\left(\dfrac{1}{(r/R)^2 - 1}\right) & |r/R| < 1 \\ 0 & \text{otherwise} \end{cases} \tag{6}$$

with different constants $p^{\max} > 0, R > 0$ for pedestrians and obstacles as well as the distance $r = \| x_i - x_j \|$ (see Fig. 4).

4. Results

Grid restrictions in CA models and indirect navigation through acceleration in the ODE models constitute the major differences in the model formulations. In three computer experiments described below, we demonstrate how pedestrian trajectories become more similar when these differences are removed with the OSM and the GNM. In the first scenario, a single pedestrian leans against a wall from where he or she moves to a target located to the right (see Fig. 5). The CA and SFM produce unnatural behavior: in the CA model, the hexagonal grid is evident. In the SFM the pedestrian moves in a wide arc and then circles around the target. In fact, depending on the numerical method, the pedestrian may never reach the goal or slow down [19]. The relaxation constant $\tau = 0.5$ (seconds) is chosen similar to values reported in [13,22]. The unnatural circling can be somewhat mitigated, at the cost of extra complexity, by attenuating the speed in a close vicinity of the target. In the OSM, the pedestrian steps away from the wall and at the same time toward the goal. The second and third steps are straight toward the goal, where the pedestrian stops. In the GNM, the pedestrian first moves a little away from the wall and then toward the target in a smooth curve parallel to the wall. There are no oscillations present. The pedestrian comes to a halt at the target. The trajectories of the OSM and the GNM look very similar.

The second scenario is inspired by a laboratory experiment by Moussaïd [22]: Trajectories of pedestrians are observed who move

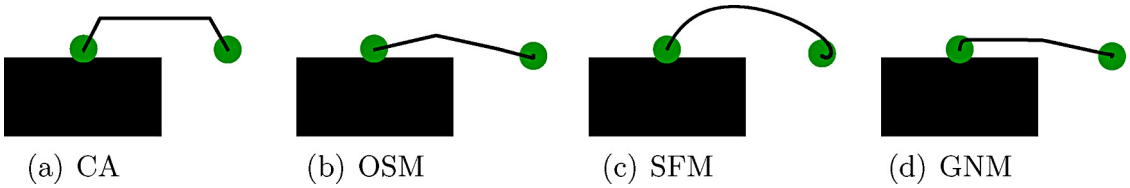

Fig. 5. Trajectories of a single pedestrian initially positioned close to a wall ($2\,m \times 1\,m$) who moves toward a target 2 m to the right. Cell width in CA is 0.39 m, maximum stride length for OSM is 0.70 m (average for speed 1.34 m s^{-1} [27]), relaxation constant τ in SFM and GNM is 0.5 s.

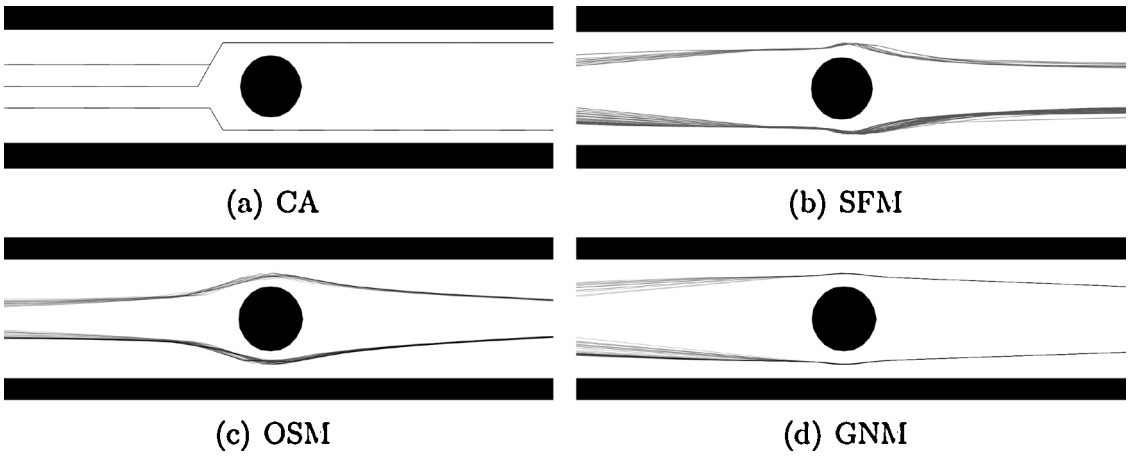

Fig. 6. Trajectories for pedestrians passing from left to right. Pedestrians walk around a pillar; the opening between the wall and the pillar is exactly the torso diameter.

around a stationary person acting as pillar in the middle of a corridor. In our computer experiment (see Fig. 6) we use a pillar, that is, an obstacle and not a virtual person. Pedestrians walk from left to right in a sequential order, so that they do not impede each other. Their start and target positions are chosen randomly at the respective ends of the corridor but not too close to the wall. The opening between the wall and a pillar in the center corresponds exactly to the torso diameter of a virtual pedestrian. Once again the trajectories of the CA look unnatural, because of the movement on the grid. On a larger scale this may become unimportant, but it makes fine resolution of bottlenecks impossible. The trajectories in the SFM are smooth. An artifact can be observed shortly after the pedestrians have passed the pillar: They bounce back from the walls. This oscillation is typical for Newtonian systems where the velocity vector is computed by integrating the acceleration vector that depends on the directional force (here along geodesics) and, in our scenario, the forces from the pillar and the wall. The OSM and GNM show similar smooth trajectories that roughly form an eye around the pillar. If the scene was magnified, individual steps would be visible in the OSM.

The third computer simulation is based on an experiment described in [21]. 180 pedestrians start 12 m away from a 1.6 m broad and 4 m long bottleneck. They all have to pass it, which leads to a congestion. Desired free-flow velocities are normally distributed with mean $1.34\,\mathrm{m\,s^{-1}}$ and standard deviation $0.26\,\mathrm{m\,s^{-1}}$, values that originate from [35]. We used the same floor field generated by the eikonal equation (Eq. (1)) for all simulations and all models.

The behavior of the pedestrians in the CA differs from that in the SFM. The coarse discretization of the CA can be seen clearly. Pedestrians tend to walk in the corners in front of the opening and even a mild compression of a crowd is difficult to realize [34]. The trajectories in the SFM are smooth, some pedestrians still move toward the corners of the first room. They form an arch in front of the opening as described by [12]. Again – behind the entrance of the smaller corridor – an artifact of the SFM can be seen: Some trajectories show an oscillating behavior. The pedestrians swing from the middle of the corridor nearer to the wall and back. As opposed to this, the trajectories of the OSM are close to the ones of the GNM. In both models, the pedestrians do not tend to walk

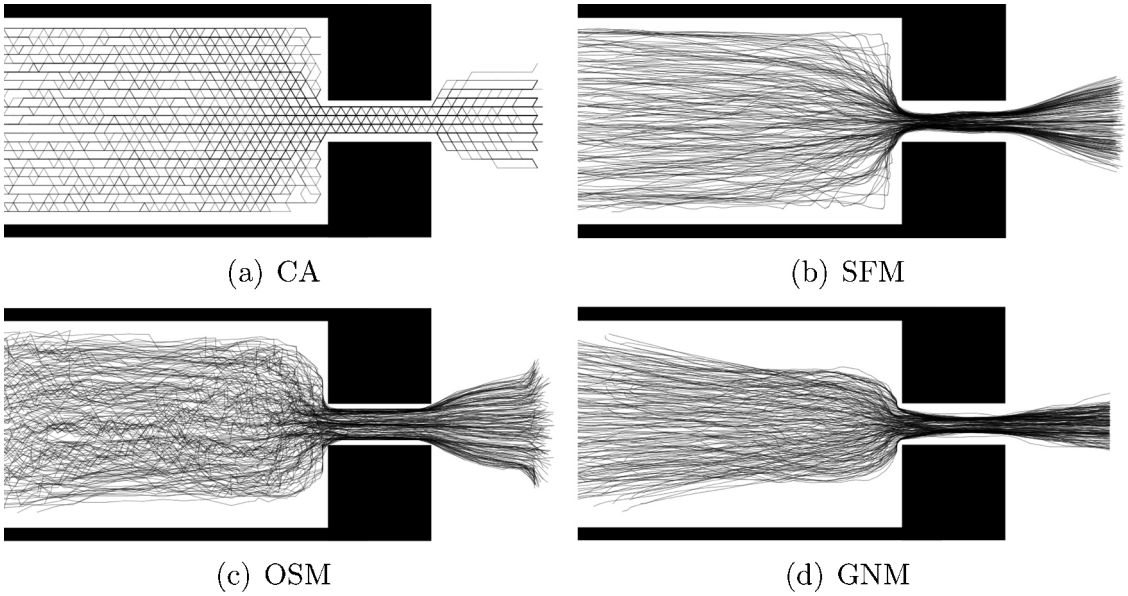

Fig. 7. Trajectories of 180 pedestrians passing from left to right through a bottleneck. Four different models for pedestrian motion are shown, all use the same floor field generated by the eikonal equation (Eq. (1)). Desired free-flow velocities are normally distributed with mean $1.34\,\mathrm{m\,s^{-1}}$ and standard deviation $0.26\,\mathrm{m\,s^{-1}}$.

in the corners and no oscillations can be observed. Nevertheless, some differences remain. In Fig. 7(c) the individual steps of the OSM are visible whereas the trajectories of the GNM are smooth. The pedestrians in the OSM do not avoid the corners completely but they are more orientated toward the smaller corridor in the middle than the pedestrians in the CA. Thus, the pedestrians in front of the opening move closer together. In the GNM, the pedestrians form a cone in front of the opening as found experimentally by [20,30,26]. The faster pedestrians overtake at the border of the crowd, which makes the cone broader. However, the overall behavior of the OSM and that of the GNM are very similar – forming a bridge between the CA and the SFM.

5. Remaining differences

The OSM with its quasi-continuous dynamic discretization of space has drawn nearer to continuous models, while the GNM has adopted the navigational ideas of successful CA-models and the OSM and integrated them in an ODE context. Nevertheless, some differences remain. In the OSM, there is no acceleration phase. Pedestrians reach their desired free flow velocity instantaneously if they are not hampered by preceding pedestrians or obstacles. In the GNM, the velocity is relaxed through an acceleration term. The density–velocity dependency in the OSM results from proper numerical calibration of the repulsive pedestrian potential, which reflects an individual's personal need for private space. This is also true for the GNM, where a specific density–velocity relation can additionally be set through direct adjustment of $v(\rho)$ in the relaxed speed equation. The trajectories of the OSM capture individual steps (Fig. 5(b)) whereas the GNM focuses on the position of the center of mass (Fig. 5(d)).

6. Conclusion and future work

Two new models for pedestrian motion were presented, one emanating from rule based CA models, but with continuous treatment of space and one based on ODEs using navigation on geodesics as in CA models. The trajectories of the new models are very similar, thus bridging the gap between the traditional modeling approaches. Closing the gap entirely may well be possible, but entails more stringent mathematical formulations and studies of the OSM to complement the present algorithmic formulation and to allow rigorous proofs.

Comparing simulation models of pedestrian movement is important in order to classify them and finally select the appropriate model for a given task. Applications vary from few pedestrians to huge crowds, from real time requirements on personal computers to massive parallel computations on mainframes. Therefore, choosing the right model with its advantages and disadvantages contributes significantly to practical applications.

It is important to further explore the model similarities and differences as well as their causes and impact. A long-term goal could be to express the GNM as the limiting case of the OSM when the discretization in time, Δt, goes to zero.

Acknowledgments

This work was funded by the German Federal Ministry of Education and Research through the project MEPKA on mathematical characteristics of pedestrian stream models (17PNT028). Support from the TopMath Graduate Center of TUM Graduate School at Technische Universität München, Germany, and from the TopMath Program at the Elite Network of Bavaria is gratefully acknowledged.

References

[1] G. Antonini, M. Bierlaire, M. Weber, Discrete choice models of pedestrian walking behavior, Transport. Res. B: Methodol. 40 (2006) 667–687, http://dx.doi.org/10.1016/j.trb.2005.09.006.
[2] J. Berg, S.J. Guy, M. Lin, D. Manocha, Reciprocal n-body collision avoidance, Springer Tracts Adv. Robot. 70 (2011) 3–19, http://dx.doi.org/10.1007/978-3-642-19457-3_1.
[3] C. Burstedde, K. Klauck, A. Schadschneider, J. Zittartz, Simulation of pedestrian dynamics using a two-dimensional cellular automaton, Phys. A: Stat. Mech. Appl. 295 (2001) 507–525, http://dx.doi.org/10.1016/S0378-4371(01)00141-8.
[4] M. Chraibi, Validated Force-based Modeling of Pedestrian Dynamics, Universität zu Köln, 2012 (Ph.D. thesis).
[5] M. Chraibi, U. Kemloh, A. Schadschneider, A. Seyfried, Force-based models of pedestrian dynamics, Netw. Heterogen. Media 6 (2011) 425–442.
[6] M. Chraibi, A. Seyfried, A. Schadschneider, Generalized centrifugal-force model for pedestrian dynamics, Phys. Rev. E 82 (2010) 046111.
[7] S. Curtis, D. Manocha, Pedestrian simulation using geometric reasoning in velocity space, in: U. Weidmann, U. Kirsch, M. Schreckenberg (Eds.), Pedestrian and Evacuation Dynamics 2012, Springer International Publishing, Switzerland, 2014, pp. 875–890, http://dx.doi.org/10.1007/978-3-319-02447-9_73.
[8] F. Dietrich, G. Koster, Gradient navigation model for pedestrian dynamics, Phys. Rev. E 89 (2014) 062801.
[9] T. Ezaki, D. Yanagisawa, K. Ohtsuka, K. Nishinari, Simulation of space acquisition process of pedestrians using proxemic floor field model, Phys. A: Stat. Mech. Appl. 391 (2012) 291–299, http://dx.doi.org/10.1016/j.physa.2011.07.056.
[10] P. Fiorini, Z. Shiller, Motion planning in dynamic environments using velocity obstacles, Int. J. Robot. Res. 17 (1998) 760–772, http://dx.doi.org/10.1177/027836499801700706.
[11] D. Hartmann, Adaptive pedestrian dynamics based on geodesics, New J. Phys. 12 (2010) 043032, http://dx.doi.org/10.1088/1367-2630/12/4/043032.
[12] D. Helbing, I. Farkas, T. Vicsek, Simulating dynamical features of escape panic, Nature 407 (2000) 487–490.
[13] D. Helbing, P. Molnár, Social Force Model for pedestrian dynamics, Phys. Rev. E 51 (1995) 4282–4286.
[14] C.M. Henein, T. White, Macroscopic effects of microscopic forces between agents in crowd models, Phys. A: Stat. Mech. Appl. 373 (2007) 694–712.
[15] A. Johansson, Constant-net-time headway as a key mechanism behind pedestrian flow dynamics, Phys. Rev. E 80 (2009) 026120, http://dx.doi.org/10.1103/PhysRevE.80.026120.
[16] A. Kirchner, H. Klüpfel, K. Nishinari, A. Schadschneider, M. Schreckenberg, Simulation of competitive egress behavior: comparison with aircraft evacuation data, Phys. A: Stat. Mech. Appl. 324 (2003) 689–697, http://dx.doi.org/10.1016/S0378-4371(03)00076-1.
[17] G. Köster, D. Hartmann, W. Klein, Microscopic pedestrian simulations: from passenger exchange times to regional evacuation, in: B. Hu, K. Morasch, S. Pickl, M. Siegle (Eds.), Operations Research Proceedings 2010: Selected Papers of the Annual International Conference of the German Operations Research Society, Springer, 2011, pp. 571–576.
[18] G. Köster, M. Seitz, F. Treml, D. Hartmann, W. Klein, On modelling the influence of group formations in a crowd, Contemp. Soc. Sci. 6 (2011) 397–414, http://dx.doi.org/10.1080/21582041.2011.619867.
[19] G. Köster, F. Treml, M. Gödel, Avoiding numerical pitfalls in social force models, Phys. Rev. E 87 (2013) 063305, http://dx.doi.org/10.1103/PhysRevE.87.063305.
[20] T. Kretz, A. Grünebohm, M. Schreckenberg, Experimental study of pedestrian flow through a bottleneck, J. Stat. Mech.: Theory Exp. 2006 (2006) P10014, http://dx.doi.org/10.1088/1742-5468/2006/10/P10014.
[21] J. Liddle, A. Seyfried, B. Steffen, W. Klingsch, T. Rupprecht, A. Winkens, M. Boltes, Microscopic insights into pedestrian motion through a bottleneck, resolving spatial and temporal variations, 2011, pp. v1, arXiv:1105.1532.
[22] M. Moussaïd, D. Helbing, S. Garnier, A. Johansson, M. Combe, G. Theraulaz, Experimental study of the behavioural mechanisms underlying self-organization in human crowds, Proc. R. Soc. B: Biol. Sci. 276 (2009) 2755–2762, http://dx.doi.org/10.1098/rspb.2009.0405.
[23] M. Moussaïd, D. Helbing, G. Theraulaz, How simple rules determine pedestrian behavior and crowd disasters, Proc. Natl. Acad. Sci. 108 (2011) 6884–6888 http://www.pnas.org/content/108/17/6884.abstract
[24] K. Nishinari, M. Fukui, A. Schadschneider, A stochastic cellular automaton model for traffic flow with multiple metastable states, J. Phys. A: Math. Gen. 37 (2004) 3101, http://dx.doi.org/10.1088/0305-4470/37/9/003.
[25] RiMEA, Richtlinie für Mikroskopische Entfluchtungsanalysen – RiMEA, 2.2.1 ed., iMEA e.V., 2009 http://www.rimea.de/
[26] A. Schadschneider, A. Seyfried, Empirical results for pedestrian dynamics and their implications for modeling, Netw. Heterogen. Media 6 (2011) 545–560 http://aimsciences.org/journals/displayArticlesnew.jsp?paperID=6445
[27] M.J. Seitz, G. Köster, Natural discretization of pedestrian movement in continuous space, Phys. Rev. E 86 (2012) 046108, http://dx.doi.org/10.1103/PhysRevE.86.046108.
[28] J.A. Sethian, A fast marching level set method for monotonically advancing fronts, Proc. Natl. Acad. Sci. 93 (1996) 1591–1595 http://www.pnas.org/content/93/4/1591.abstract
[29] J.A. Sethian, Level Set Methods and Fast Marching Methods: Evolving Interfaces in Computational Geometry, Fluid Mechanics, Computer Vision, and Materials Science, Cambridge University Press, 1999.
[30] A. Seyfried, B. Steffen, A. Winkens, T. Rupprecht, M. Boltes, W. Klingsch, Empirical data for pedestrian flow through bottlenecks, in: C. Appert-Rolland, F.

Chevoir, P. Gondret, S. Lassarre, J.P. Lebacque, M. Schreckenberg (Eds.), Traffic and Granular Flow 2007, Springer, Berlin, Heidelberg, 2009, pp. 189–199, http://dx.doi.org/10.1007/978-3-540-77074-9_17.
[31] Z. Shiller, F. Large, S. Sekhavat, Motion planning in dynamic environments: obstacles moving along arbitrary trajectories, in: IEEE International Conference on Robotics and Automation, vol. 4, 2001, pp. 3716–3721, http://dx.doi.org/10.1109/robot.2001.933196.
[32] I. von Sivers, G. Köster, How stride adaptation in pedestrian models improves navigation, 2014, pp. v1, arXiv:1401.7838.
[33] A. Treuille, S. Cooper, Z. Popović, Continuum crowds, ACM Trans. Graphics (SIGGRAPH 2006) 25 (2006) 1160–1168, http://dx.doi.org/10.1145/1141911.1142008.
[34] J. Was, R. Lubas, Adapting social distances model for mass evacuation simulation, J. Cell. Automata 8 (5–6) (2013) 395.
[35] U. Weidmann, Transporttechnik der Fussgänger, volume 90 of Schriftenreihe des IVT, 2 ed., Institut für Verkehrsplanung, Transporttechnik, Strassen- und Eisenbahnbau (IVT) ETH, Zürich, 1992, http://dx.doi.org/10.3929/ethz-a-000687810 http://e-collection.library.ethz.ch/view/eth:5929
[36] P. Zhang, X.X. Jian, S.C. Wong, K. Choi, Potential field cellular automata model for pedestrian flow, Phys. Rev. E 85 (2012) 021119, http://dx.doi.org/10.1103/PhysRevE.85.021119.
[37] X. Zheng, T. Zhong, M. Liu, Modeling crowd evacuation of a building based on seven methodological approaches, Building Environ. 44 (2009) 437–445 http://www.sciencedirect.com/science/article/pii/S0360132308000577

Felix Dietrich (B.Sc Scientific Computing, B.Sc Mathematics) is a researcher at the Munich University of Applied Sciences. He focuses on numerical analysis of multiple scale systems, specifically pedestrian flows.

Prof. Dr. Gerta Köster teaches mathematics and computer science at the Munich University of Applied Sciences. She leads the research group for modelling and simulation of the behavior of people in crowds.

Michael Seitz (B.Sc Computer Science, M.Sc. Statistics) is a researcher at the Munich University of Applied Sciences. He focuses on the cognitive heuristics used by pedestrians in crowds.

Isabella von Sivers (B.Sc Scientific Computing, M.Sc. Mathematics) is a researcher at the Munich University of Applied Sciences. She focuses on models for affiliative behavior and social identity.